A Review of the Overflow of Inflatable Flexible Membrane dams*

H Chanson, ME, ENSHMG, INSTN, PhD (Cant), EurIng, MIEAust, MIAHR
Senior Lecturer, Fluid Mechanics, Hydraulics and Environmental Engineering
Department of Civil Engineering, The University of Queensland, Brisbane QLD 4072, Australia.

SUMMARY *Inflatable flexible membrane dams (IFMD) have been used for the past 40 years in river and coastal engineering applications. Despite an increasing interest for IFMD, little information is available on the hydraulic performances of IFMD during overflow periods. Overflow situations may occur with deflated or inflated membranes. Both situations are described. It has been recognised that overflowing waters may induce some form of fluid-structure interactions, which might cause vibrations of the IFMD structure, leading to damage or destruction of the membrane. Several flow instability mechanisms are reviewed and the associated hazards are discussed. For overflow situations above inflated dams, new flow calculations are detailed and the results give new information on the wall pressure distribution along the downstream face of the dam. A mechanism of cavitating flow separation is also explained.*

NOTATION

The following symbols are used in this paper :

- D inflatable dam height (m) above the floor;
- d flow depth (m) measured perpendicular to the channel bottom;
- d_c critical flow depth (m) : for a rectangular channel: $d_c = \sqrt[3]{q_w^2 / g}$
- d_1 upstream flow depth (m);
- d_2 downstream flow depth (m);
- F Froude number based on the circular cylinder radius: $F = V / \sqrt{g * R}$
- F_c critical Froude number based on the circular cylinder radius: $F_c = V_c / \sqrt{g * R}$
- Fr Froude number;
- Fr_1 upstream Froude number: $Fr_1 = q_w / \sqrt{g * d_1^3}$
- g gravity constant : g = 9.80 m/s² in Brisbane, Australia;
- H total head (m);
- H_1 upstream total head (m);
- P pressure (Pa);
- P_{atm} atmospheric pressure (Pa);
- P_{hyd} hydrostatic pressure (Pa);
- P_{infl} inflation pressure (Pa);
- P_s absolute pressure (Pa) at the downstream surface of the cylinder;
- P_v vapour pressure (Pa);
- q_w water discharge per unit width (m²/s);
- R 1- radius of curvature (m) of the inflated membrane; 2- radius (m) of circular cylinder;
- t_d thickness (m) of deflated membrane;
- V velocity (m/s);
- W channel width (m); for a channel of irregular cross-section, W is the free-surface width;
- Δz drop height (m) or weir height;
- ϕ angular position on the inflated dam (angle between the vertical and the local position);
- ϕ_{sep} angular position of the separation point;
- ρ_w water density (kg/m³);
- σ_c critical cavitation number at which cavitation starts to appear;

Subscript

- c critical flow conditions;
- w water flow;
- 1 upstream flow conditions;
- 2 downstream flow conditions;

Abbreviations

- IFMD inflatable flexible membrane dam;
- NCF near-critical flow.

1 INTRODUCTION

Inflatable flexible membrane dams (IFMD), also called rubber dams, have been used for the past 40 years in rivers and estuaries. In open channels, they are commonly used to raise water levels, to increase water storage or to prevent chemical dispersion. The interest in inflatable dams is increasing because of the ease of placement. Such structures can be installed during later development stages : e.g., to increase the performance of existing facilities (IFMD placed along spillway crest) (fig. 1).

Despite an increasing interest for IFMD, little information is available on the hydraulic performances of IFMD during overflow periods. One researcher (ANWAR 1967) investigated the discharge characteristics and few studies (SHEPHERD et al. 1969, BINNIE et al. 1973, CHANSON 1996) discussed the effects of overflow on the downstream face of the inflated dam. OGIHARA and MURAMATSU (1985)

* Paper C/97005 was first submitted to IEAust on 5/3/97. Paper accepted 11/8/97.

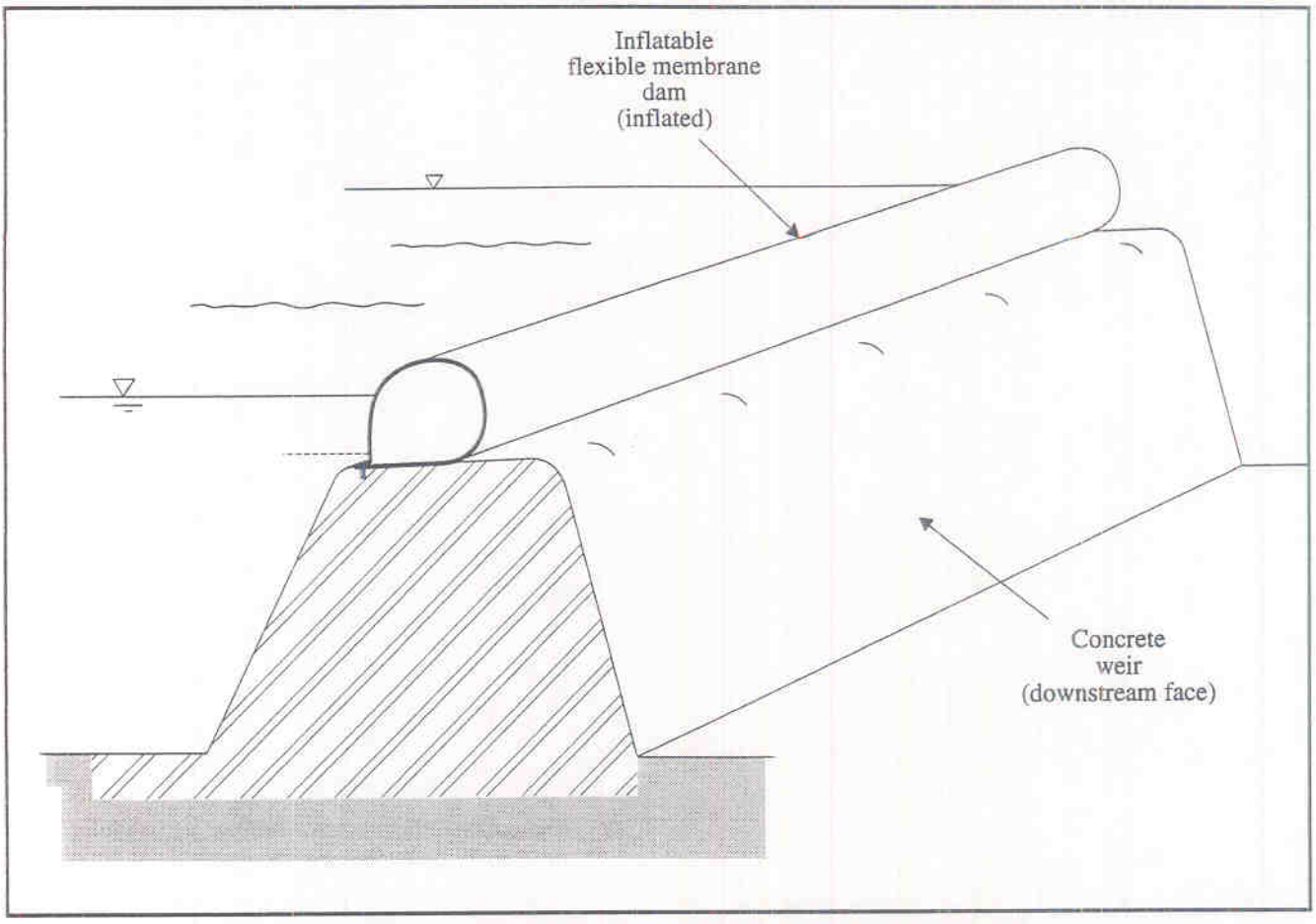

Figure 1 Inflated flexible membrane dam at the crest of a concrete weir

showed the potential for vibrations at large overflows and recommended the installation of a deflector on the downstream face.

Discharging waters over IFMD may induce some form of fluid-structure interaction, which might cause vibrations of the IFMD structure. Such instabilities might damage or destroy the inflatable dam and they are not acceptable.

In this paper, the overflow of rubber dams is considered. Initially hydrodynamics problems during the overflow of deflated membranes are reviewed. Then the hydraulic characteristics of overflowing waters on inflated dams are described. A new analytical method is developed to predict the adherence of the nappe on the membrane and flow conditions for nappe separation are described.

2 OVERFLOW ABOVE DEFLATED FLEXIBLE MEMBRANE DAM

2.1 Introduction

When the flexible membrane is deflated, the waters flow over the membrane lying flat on the bed (of the channel or of the crest) (fig. 2) and head losses associated with the deflated membrane must be at a minimum to optimise the hydraulic performances of the channel or of the crest.

Some of the following hydrodynamic processes might take place and lead to erosion, damage or destruction of the membrane : hydraulic jump induced vibrations, near-critical flow induced vibrations, wake induced vibrations (i.e. vortex shedding), and debris erosion.

Deflated rubber membranes can sustain large positive pressure, but they cannot sustain negative pressures (instantaneous and mean pressures) nor bottom shear stress in directions normal or opposite to the flow direction.

2.2 Hydraulic jump induced vibrations

In open channel flow, a hydraulic jump is the sudden transition from a rapid (supercritical) to a tranquil (subcritical) flow. It is characterised by the development of large-scale turbulence and considerable energy dissipation. Below the roller, the mean bottom pressure is quasi-hydrostatic but large pressure fluctuations are observed (HAGER 1992). Experimental investigations showed that the instantaneous maximum pressures on the floor are about:

$$P_{hyd} + 0.6 * \rho_w * \frac{V_1^2}{2} \text{ instantaneous maximum pressure below a hydraulic jump} \quad (1a)$$

and the instantaneous minimum pressures are nearly:

$$P_{hyd} + 0.4 * \rho_w * \frac{V_1^2}{2} \text{ instantaneous minimum pressure below a hydraulic jump} \quad (1b)$$

where P_{hyd} is the local hydrostatic pressure, ρ_w is the water density and V_1 is the upstream flow velocity. Note that the

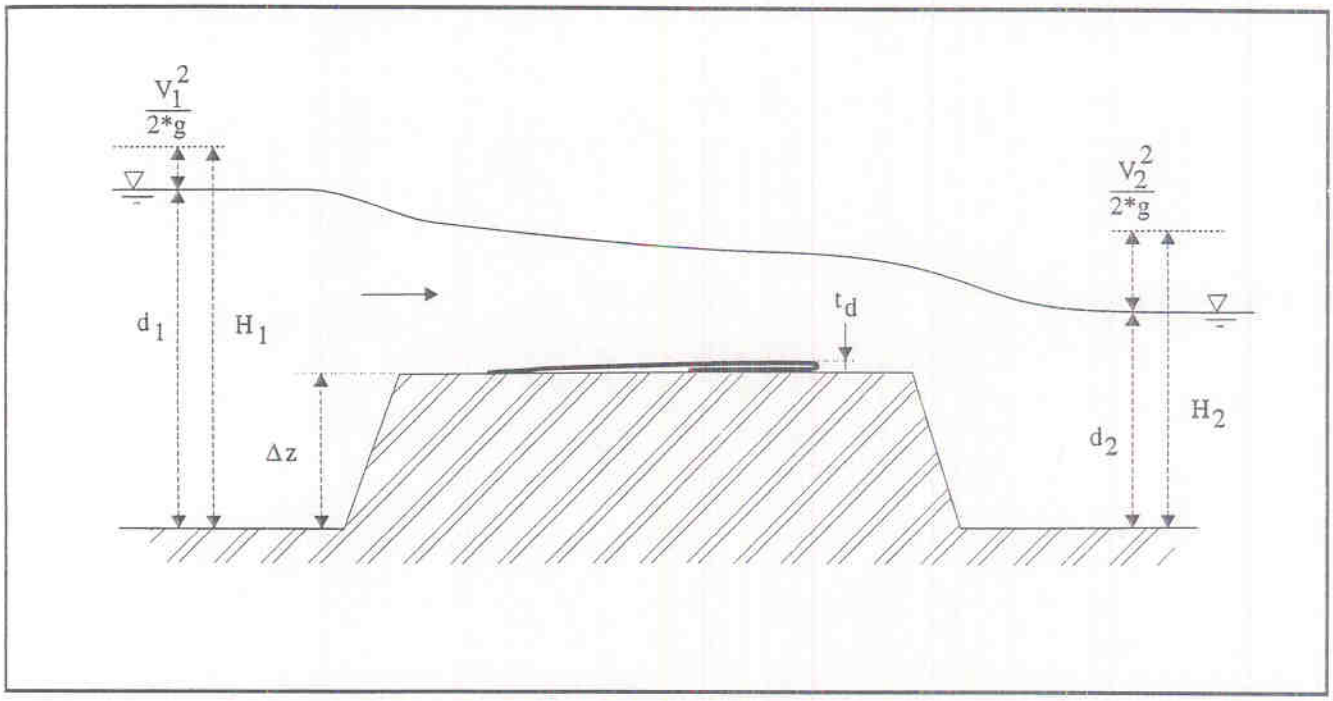

Figure 2 Overflow above a deflated rubber dam

extreme minimum pressures (eq. (1b)) might become negative and could lead to uplift forces. Further hydraulic jumps are characterised by large bottom shear stresses and large shear stress fluctuations (e.g. IMAI and NAKAGAWA 1995).

Practically, a deflated flexible membrane dam (IFMD) should **never** be located below or next to a hydraulic jump because the instantaneous uplift pressures and large fluctuating shear stresses would cause a rapid destruction of the membrane.

2.3 Near-critical flow induced vibrations

Near-critical flows (NCF) are defined as flow situations characterised by the occurrence of critical or nearly-critical flow conditions over a "reasonably-long" distance and period time. At critical flow conditions[1], very small changes of energy (e.g. caused by boundary irregularity, by turbulence or by upstream disturbance) can induce very large changes of flow depth. As a result, near-critical flows (i.e. undular flows) are characterised by the development of large free-surface undulations, associated with non-hydrostatic bottom pressures and fluctuating bottom shear stresses. Below the wave crests the mean bottom pressures are typically less than hydrostatic and flow separation might take place in some particular cases (e.g. CHANSON 1995, MONTES 1986). This might lead to uplift on the membrane. Further the bottom shear stress is not uniformly distributed and negative bottom shear stress might take place in regions of flow separation.

CHERVET (1984) described the rapid abrasion of an inflatable dam caused by near-critical flow conditions (Glatt river, Switzerland). His study highlighted two modes of vibrations : wave propagating along the membrane in the downstream direction, and vertical flip of the downstream edge of the deflated membrane (fig. 3).

[1] The flow conditions such that the specific energy is at a minimum are called the critical flow conditions

In summary, inflatable flexible membrane dams must not be operated with near-critical flow conditions. If these flow conditions cannot be avoided (e.g. because of tailwater flow conditions), a partial inflation of the IFMD might be considered to modify the flow conditions above the dam.

Occurrence of near critical flows

In practice, near-critical flows are encountered when the Froude number ranges typically between 0.3 to 3. The author (CHANSON 1995) developed recently a comprehensive review of several near-critical flow situations.

The occurrence of near-critical flow conditions is related to the upstream and downstream flow conditions, to the weir height or drop height Δz, and eventually to the deflated membrane thickness t_d for low flow depths (Table I). The results shown in Table I may assist to check the proper overflow operation of deflated IFMD.

2.4 Wake induced vibrations

When deflated, the flexible membrane lies flat on the floor. Usually anchors and casing are streamlined with the floor. Even in the best position, the thickness of the membrane induces a wake flow region downstream of the membrane edge (fig. 4). The wake is a turbulent flow region in which the velocity redistribution leads to a modification of the pressure field (i.e. non-hydrostatic pressure distribution) and sometimes to significant pressure fluctuations (SCHLICHTING 1979). This process, called vortex shedding, might cause the destabilisation of the deflated membrane (i.e. wake-induced vibrations).

In practice, the deflated membrane (lying on the floor) may be streamlined by a recess in the concrete floor. Usually, economical considerations lead to some form of recess for the anchorage but the membrane lies flat on the floor. In

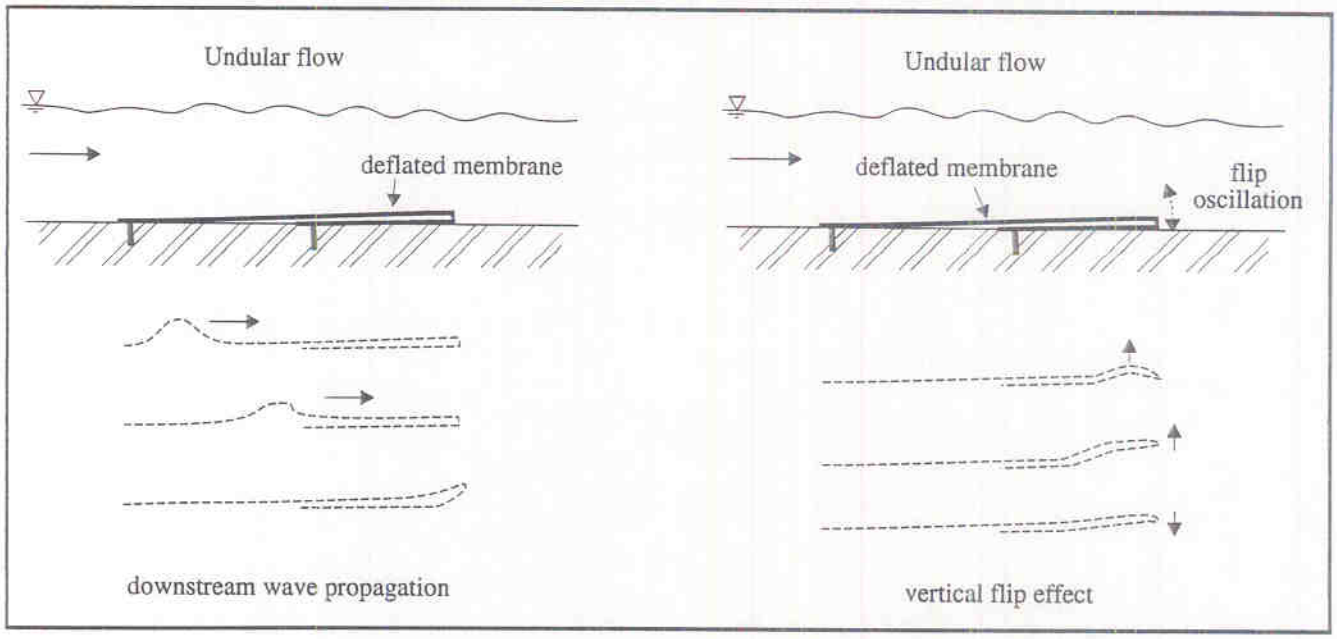

Figure 3 Vibration modes of deflated membrane below near-critical flow (after CHERVET's (1984) photographs)

Table I
Near-critical flow conditions in rectangular channels

Flow situation/Reference (1)	Flow conditions (2)	Remarks (3)
Flat channel flow CHANSON (1996)	$0.3 \leq Fr_1 \leq 3$	Thin deflated membrane (i.e. $t_d/d_1 << 1$). Based upon Chanson's (1995) results
	$Fr_1^{4/3} + 2 * Fr_1^{-2/3} \leq 5 + 2 * \frac{t_d}{d_c}$	Thick deflated membrane. Valid for both sub and supercritical flows
Broad-crested weir flow CHANSON (1995)	$\frac{H_1 - d_1}{\Delta z} \leq 0.1$	Re-analysis of laboratory experiments of HAGER and SCHWALT (1994) and studies of BOS (1976) and GOVINDO RAO and MURALIDHAR (1963)
Backward facing step *Rounded drop* SHARP (1974)	$Fr_1 < 2.2$ for $\Delta z/d_1 = 2$ $Fr_1 < 4$ for $\Delta z/d_1 = 3.5$	Laboratory experiments
HAGER and kawagoshi (1990)	$Fr_1 < 2.44 + 0.28 * \frac{\Delta z}{d_1}$	Laboratory experiments $1.4 < \Delta z/d_1 < 9$
Abrupt drop CHOW (1959)	$\frac{1}{2} * \frac{d_2}{d_1 - d_2} * \left(1 - \left(\frac{d_2}{d_1} - \frac{\Delta_z}{d_1}\right)\right)^2 < Fr_1^2 <$ $\frac{1}{2} * \frac{d_2}{d_1 - d_2} * \left(\left(1 + \frac{\Delta z}{d_1}\right)^2 - \left(\frac{d_2}{d_1}\right)^2\right)$	

Notes: d_c: critical flow depth; Fr_1: upstream Froude number

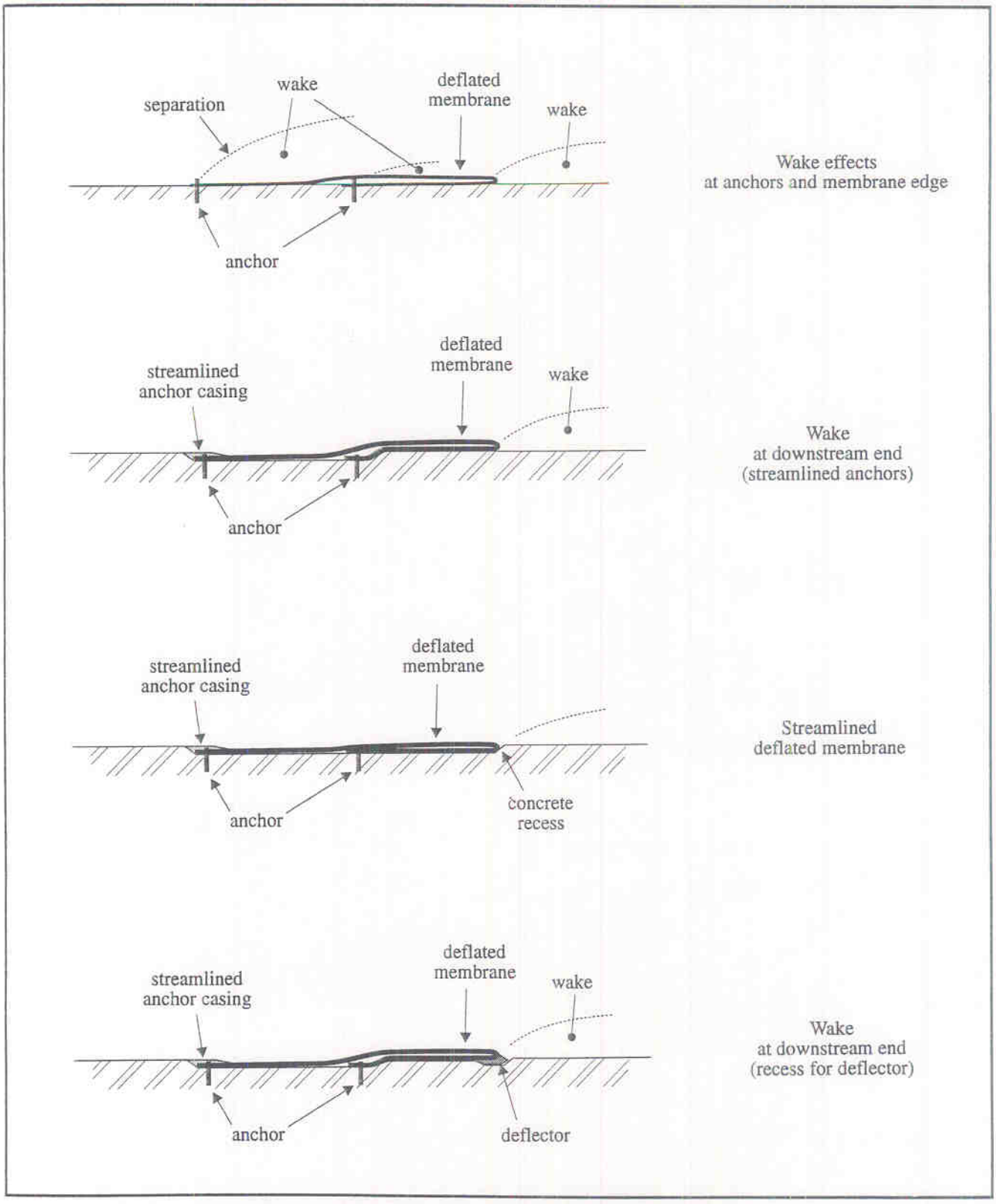

Figure 4 Wake regions downstream of deflated membranes

cases with a thick downstream edge (e.g. caused by a fin), a special recess in the floor must be prepared to streamline the downstream end (fig. 4). This disposition minimises the floor discontinuity (protuberance or gap) caused by the device and reduces the vortex shedding effects.

2.5 Debris erosion

Erosion of the membrane by debris might result from recurrent abrasion and debris impacts. A protective casing or steel gate can be considered to reduce or prevent membrane abrasion (e.g. Omata weir, Japan). Debris impact is not often taken into account and the impact process is still poorly understood. Nevertheless the impact of debris can be significant. In one case (Ngalimbiu bridge, Solomon islands), substantial damage to concrete bridge piers was reported with plastic hinges in the pier portals, and it is believed that debris impacts contributed to the bridge failure (BOYCE 1987).

With flexible membranes, impact by large debris (e.g. branch, tree, log, ice) must be avoided at any cost because of the risk of puncture. A hard cover of the deflated membrane might be required in case of potential debris impacts. Alternatively rigid dams or gates must be selected in place of IFMD.

2.6 Discussion

In summary, deflated membranes must not be located in flow regions with low-pressures (in terms of both mean and instantaneous pressures) which would apply an uplift motion on the membrane. The stability of deflated flexible membrane dams can be increased by placing the IFMD in a region of larger bottom pressures (i.e. larger than hydrostatic). Larger bottom pressures are achieved in regions of converging flow with smooth-curved boundaries. Such a recommendation leads to the installation of the membrane on inclined-upward bottom[2]. For IFMD installed at the crest of concrete weirs, it is common practice to design the crest with a 3-degree upward deflection . In other situations, the upwards slope angle must be appropriately selected as a function of the channel geometries, discharge, upstream flow conditions and IFMD dimensions. Note that the upstream flow conditions might affect significantly the required design. For example, if the upstream flow conditions are very turbulent, larger (than usual) values of upward bottom angle are recommended.

3 OVERFLOW OF INFLATED RUBBER DAMS

3.1 Presentation

Several researchers indicated vibration problems during overflow above inflated IFMD. A summary of model and prototype observations is given in Table II. In Table II, column 2 describes flow conditions for a safe operation of inflated IFMD.

Considering a fully-inflated (air-inflated) IFMD, experimental and computational investigations (e.g. ANWAR 1967) showed that the downstream face of the membrane follows closely the shape of a circular cylinder. For the sake of simplicity, we shall consider the analogy with the overflow above a two-dimensional circular cylinder (fig. 5).

Basic ideal-fluid flow calculations (see appendix A) provide an estimate of the wall pressure on the downstream face. In dimensionless term, it yields :

Table II
Observations and recommendations to prevent vibration cases during overflow above inflated IFMD (without fin)

Reference (1)	Safe operation of IFMD (2)	Comments (3)
ANWAR (1967)	$\frac{H_1 - \Delta z_1}{D} < 1.25$	Laboratory study. 2-D model. Air-filled membrane. Horizontal crest. W = 0.610m. D = 0.229 m. Δz = 0.076m.
SHEPHERD et al. (1969)	$\frac{H_1 - \Delta z_1}{D} < 4$	1:50 laboratory model of Koombooloomba dam spill way. 3-D model. Curved spillway crest. Water filled membrane. Model: D = 0.0305m.
BINNIE et al. (1973)	$\frac{H_1 - \Delta z_1}{D} < 1.64$	Prototype failure. 3 water filled membranes. Flat crest. W = 63.7 to 76.2m. D = 3.05m.
OGIHARA and MURAMATSU (1985)	$\frac{H_1}{D} < 1.2$	Laboratory tests. Air-filled membrane. W = 3m. D = 0.2m. Δz = 0.
	$\frac{H_1}{D} < 1.3$	Laboratory tests. Water-filled membrane. W = 3m. D = 0.2m. Δz = 0.
TAKASAKI (1989)	$\frac{H_1}{D} < 1.3$	Omata weir model tests. Air-filled membrane. Δz = 0.
ECONOMIDES (1993)	$\frac{H_1}{D} < 1.4$	Review of manufacturers' recommendations
ECONOMIDES and WALKER (1994)	$\frac{H_1}{P_{infl} / (\rho_w * g)} < 1.15$	Laboratory tests. Air-filled membrance. Model 1: W = 0.61m, D = 0.0635m (fully inflated), Dz = 0). Model 2: W = 1.83m, D = 0.0635m, Δz = 0.
Present study	$\frac{H_1 - D}{R} < \frac{3}{\sigma_c} * \frac{P_{atm} - P_v}{\rho_w * g * R} - 6$	Overflow above circular cylinder. Theoretical calculations. Conditions to prevent cavitating separation.

Notes: D: dam height; H_1: upstream total head; P_{infl}: inflation pressure; P_v: vapor pressure; W: channel width; Δ_{z1}: weir height; σ_c: cavitation parameter.

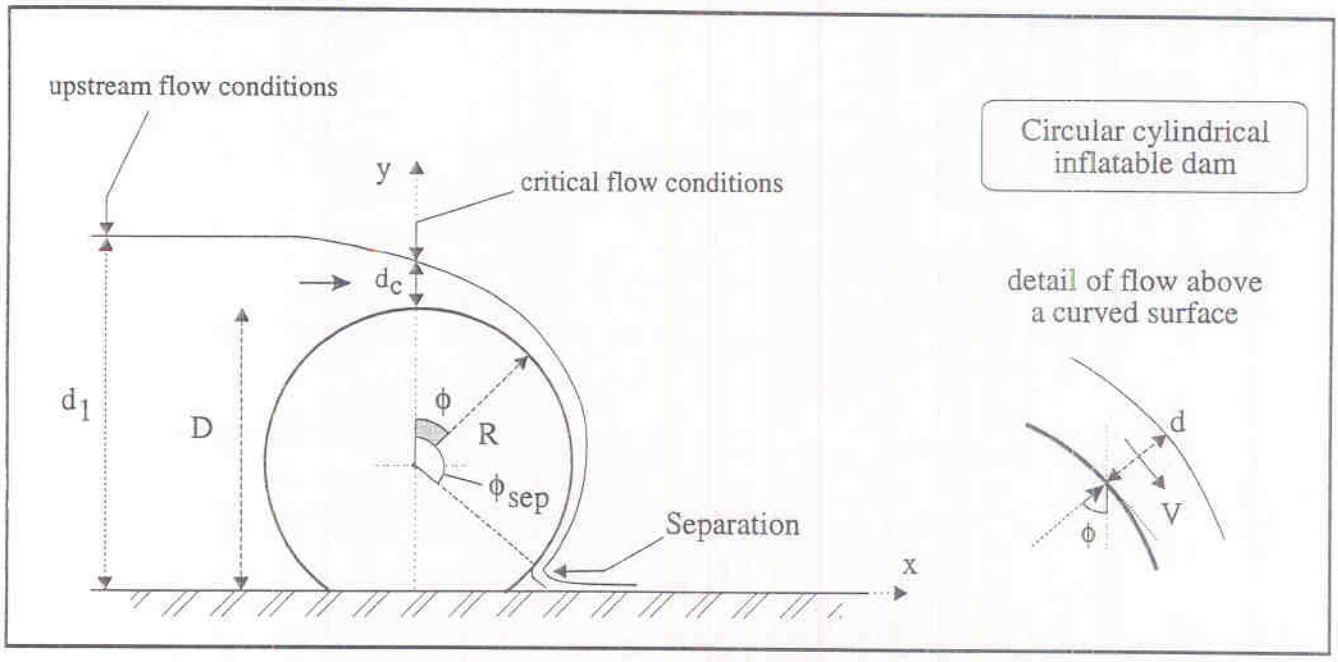

Figure 5 Overflow above a circular (inflated) IFMD

$$\frac{P_{atm} - P_s}{\rho_w * g * R} = \frac{d}{R} * \left(F^2 - \cos\phi * \left(1 + \frac{d}{2 * R} \right) \right) \quad (2)$$

where P_s is the absolute pressure at the surface of the cylinder, P_{atm} is the atmospheric pressure, ρ_w is the water density, g is the gravity constant, R is the radius of curvature, d is the nappe thickness, $F = V / \sqrt{g * R}$, and ϕ is the angular position with $\phi = 0$ at the crest (fig. 5).

The dimensionless flow depth d/R and Froude number F may be deduced from the continuity and momentum equations :

$$\frac{d}{R} = \frac{d_c}{R} * \sqrt{\frac{1}{1 + 2 * \frac{1 - \cos\phi}{F_c^2}}} \quad (3)$$

$$F = \sqrt{F_c^2 + 2 * (1 - \cos\phi)} \quad (4)$$

where $F_c = V_c / \sqrt{g * R}$, d_c is the critical flow depth, V_c is the critical flow velocity, D is the dam height and H_1 is the upstream total head (fig. 5).

Typical dimensionless pressure distributions are shown in figure 6 for various overflow situations.

Equation (2) predicts a sub-atmospheric wall pressure (i.e. $P_s < P_{atm}$) when the centrifugal effect becomes larger than the gravity component. Further the adherence pressure ($P_{atm} - P_s$) increases along the downstream face of the dam as the flow is accelerated. In the lower quadrant (i.e. $90 < \phi < 180$ deg.), the gravity force component adds to the centrifugal effect.

3.2 Nappe adherence and separation

Equations (2) to (5) imply that the suction pressure ($P_{atm} - P_s$) increases with increasing distance along the downstream wall (fig. 6). The absolute fluid pressure at the wall cannot however fall below the vapour pressure P_v. For $P_s = P_v$, the water (next to the wall) will vaporise and separation will occur. This process is called cavitation. In practice, cavitation may take place at higher absolute pressures than P_v. Experimental observations suggest that cavitation occurs for :

$$\frac{P_{atm} - P_v}{0.5 * \rho_w * V^2} < \sigma_c \quad \text{Cavitating flow} \quad (5)$$

where σ_c is a critical cavitation number at which cavitation starts to appear in the flow, being typically about 0.5 to 1 (e.g. KNAPP et al. 1970).

For the overflow above a circular dam face (fig. 5), the occurrence of cavitating nappe separation can be predicted by equations (2) and (5). Nappe separation by cavitation occurs for :

$$\cos\phi_{sep} = 1 - \left(\frac{1}{\sigma_c} * \frac{P_{atm} - P_v}{\rho_w * g * R} - \frac{1}{2} * \frac{d_c}{R} \right) \quad (6)$$

where ϕ_{sep} is the separation location (fig. 5). Equation (6) has zero or one practical solution (i.e. $0 < \phi < 180$ deg.). On figure 7, equation (6) is plotted for several dimensionless overflow ratio d_c/R.

Note that figure 7 implies that the risk of cavitating separation increases with the IFMD radius. Large IFMD structures are more susceptible to cavitation and flow separation than smaller structures, and in particular IFMD scale models.

3.3 Discussion

The author wishes to highlight clearly that the development is based upon several assumptions : the inflated IFMD shape is assumed circular (radius R), surface tension effect is neglected, friction loss and turbulent loss are neglected, the effects of developing shear flow along the membrane are neglected and the fluid is assumed incompressible and frictionless.

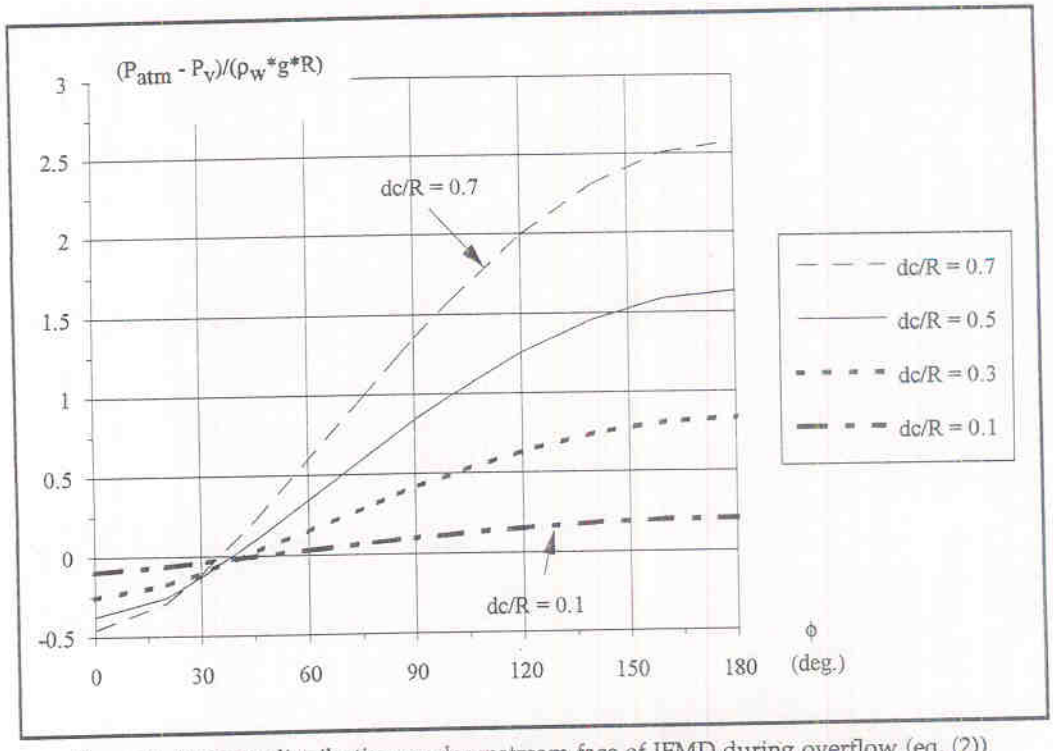

Figure 6 Pressure distribution on downstream face of IFMD during overflow (eq. (2))

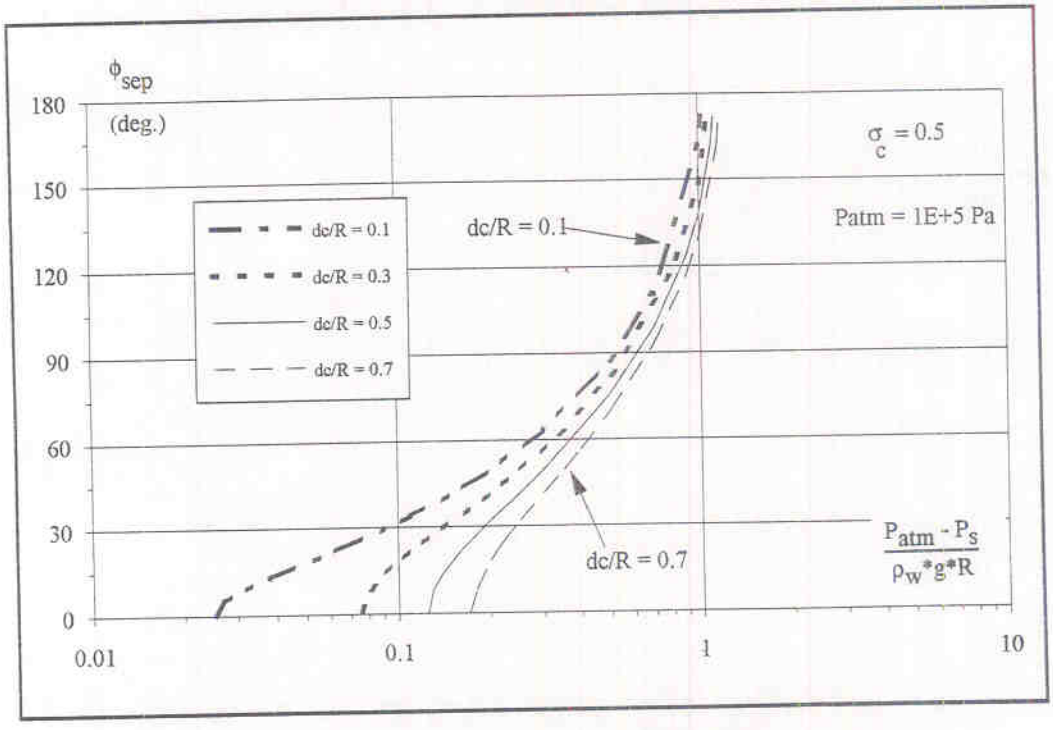

Figure 7 Flow separation location (eq. (6)) for $\sigma_c = 0.5$ and $P_{atm} = 1E+5$ Pa

Nevertheless the results give new information. First equation (5) and (6) indicate the potential for nappe separation by cavitation. Cavitation is defined as the formation of vapour bubbles and vapour pockets within a homogeneous liquid caused by excessive stress (FRANC et al. 1995) and it characterised by damaging erosion, additional noise, vibrations and energy dissipation. For an inflated IFMD, cavitation (and cavitating separation) must be avoided.

Note that the cavitating nappe separation process must be scaled by a Froude law and by a cavitation parameter law (eq. (6)). If the fluids (air and water) are at same temperature and reference pressure in both model and prototype, true similitude of the separation process is not possible : e.g. a scale model could not predict the cavitating operation of a prototype. True similitude could be achieved only using a hydrodynamic tunnel facility to keep constant $(P_{atm} - P_v)/(\rho_w * g * R)$ between model and prototype.

In practice, the adherence of the nappe on the membrane might lead to flow instability at the base of the nappe (i.e. next to the separation position) or, eventually, to an "explosive" separation by cavitation. It is nowadays common practice to design inflatable flexible membrane dams with a fin on the downstream face, acting as a deflector. Although the deflector arrangement has some advantages, other flow in-

stabilities might take place. The author (CHANSON 1996) has developed a complete review and proposed guidelines for the optimum location of the deflector.

4 CONCLUSION

Inflatable flexible membrane dams are commonly used to raise water levels, to increase water storage or to prevent chemical dispersion. The present study has reviewed various aspects of overflow above inflatable dams. Both deflated and fully-inflated configurations have been considered. The fluid-structure interactions have been detailed. The report has highlighted several forms of fluid-structure instabilities which might take place (Table III), and guidelines are suggested to avoid such flow instabilities.

During the design of IFMD and during their operation, the flow instability situations must be considered, and efforts must be made to avoid these. They might lead to the destruction of the structure.

For overflow situations above inflated dams, the overflowing nappe adheres to the downstream wall (i.e. Coanda effect). Ideal-fluid flow calculations of suction pressure distribution and risk of nappe separation have been developed. It has been shown that a possible (and explosive) mechanism of nappe separation is cavitation.

Additional work, and in particular some physical modelling, is required to obtain new information on the various hydrodynamic instabilities.

5 ACKNOWLEDGEMENTS

The author acknowledges the financial support of Queensland Rubber Company (Australia) which initiated his interest in the topic.

6 REFERENCES

1. Anwar HO. Inflatable dams. Jl of Hyd Div, ASCE, 1967;93(HY3):99-119.
2. Binnie GM, Thomas AR and Gwyther JR. Inflatable Weir used during Construction of Mangla Dam. Proc Instn Civ Eng, Part 1, 1973;54:625-639. Discussion, Part 1, 1974;56:189-194.
3. Bos MG. Discharge Measurement Structures. Publication No 161. Delft Hydraulic Laboratory, Delft, The Netherlands, 1976 (also Publication No 20, ILRI, Wageningen, The Netherlands).
4. Boyce WH. Cyclone Namu and the Ngalimbiu Bridge — Did it fall or was it pushed? Queensland Div Tech Paper, IEAust, 1987;Vol28(20):13-18.
5. Chanson H. Flow Characteristics of Undular Hydraulic Jumps. Comparison with Near-Critical Flows. Report CH45/95. Dept of Civil Engineering, University of Queensland, Australia, June 1995.

Table III
Potential fluid-structure instabilities during overflow above IFMD

Mode of operation (1)	Fluid structure instability (2)	Hydraulic process (source of instability) (3)	Design/Remedy (3)
Deflated IFMD			
	Hydraulic jump induced vibrations	Hydraulic jump above or next to deflated membrane	Avoid deflated IFMD below or next to hydraulic jump.
	NCF induced vibrations	Near-critical flow situation in in the vicinity of deflated membrane	Avoid IFMD below or next to near-critical flow.
	Wake induced vibrations	Vortex shedding in wake regions caused by membrane protuberance into the flow and downstream end of membrane	Minimise vortex shedding by streamlining the outer shape of deflated membrane, reducing protuberance into the flow.
	Debris erosion	Abrasion by debris overflow and impact by debris	Casing, pneumatic gate or or steel gate. Consider alternative design.
Inflated IFMD without deflector	Nappe adherence instability	Adherence of overflowing nappe on downstream face of membrane caused by Coanda effect and gravity	Installation of deflector
	NCF induced vibrations	Near critical flow situation immediately downstream of IFMD	Avoid IFMD below or next to near-critical flow.
	Debris erosion	Debris overflow (abrasion, impact)	Consider alternative design

6. Chanson H. Some Hydraulic Aspects during Overflow above Inflatable Flexible Membrane Dam. Report CH47/96. Dept of Civil Engineering, University of Queensland, Australia, May 1996.

7. Chervet A. Model-Prototype of the Defective behaviour of an Inflatable Dam. In: H Kobus, ed. Proc Intl Symp on Scale Effects in Modelling Hydraulic Structures, IAHR, Esslingen, Germany, 1984.

8. Chow VT. Open Channel Hydraulics. New York, USA: McGraw-Hill International, 1959.

9. Economides TA. Experimental Investigation on the Dynamics of Inflatable Dams. Virginia, USA: Polytech Inst & State Univ, 1993. Thesis.

10. Economides TA and Walker DA. (1994)Non-Intrusive Experimental Setup for Inflatable Dam Models. In: A Clifford, ed. Proc of Symp on Fundamentals and Advancements in Hydraulic Measurements and Experimentation, ASCE, 1994:500-508.

11. Govinda Rao NS and Muralidhar D. Discharge Characteristics of Weirs of Finite-Crest Width. Jl La Houille Blanche, 1963(5):537-545.

12. Hager WH. Energy Dissipators and Hydraulic Jump. Dordrecht, The Netherlands: Kluwer Academic Publ, Water Science and Technology Library, 1992;8.

13. Hager WH and Kawagoshi N. Hydraulic Jumps at Rounded Drop. Proc Instn Civ Engrs, Part 2, 1990;89:443-470.

14. Hager WH and Schwalt M. Broad-Crested Weir. Jl of Irrigation and Drainage Engrg, ASCE, 1994;120(1):13-26. Discussion;12(2):222-226.

15. Imai S and Nakagawa T. On Longitudinal and Transverse Variation of Bed Shear Stress on the Wetted Perimeter of a Sloped Rectangular Open Channel in a Hydraulic Jump. Acta Mechanica, 1995;111:141-150.

16. Knapp RT, Daily JW and Hammitt FG. Cavitation. New York, USA: McGraw-Hill Book Company, 1970.

17. Montes JS. A Study of the Undular Jump Profile. Proc of the 9th Australasian Fluid Mechanics Conference AFMC, Auckland, New Zealand, 1986:148-151.

18. Ogihara K and Maramatsu T. Rubber dam: Causes of Oscillation of Rubber Dams and Countermeasures. Proc. 21st IAHR Congress, Melbourne, Australia, 1985:600-604.

19. Schlichting H. Boundary Layer Theory, 7th edition. New York, USA: McGraw-Hill, 1979.

20. SHARP JJ. Observations on Hydraulic Jumps at Rounded Steps. Jl of Hyd Div, ASCE, 1974;100(HY6):787-795.

21. Shepherd EM, McKay FA and Hodgens VT. The Fabridam Extension on Koombooloomba Dam of the Tully Falls Hydro-Electric Power Project. Jl Instn of Eng, Australia, 1969;41:1-7.

22. Takasaki M. (1989). The Omata Inflatable Weir, at the Kawarabi Hydro Scheme, Japan. Intl Water Power & Dam Construction, 1989;41(11):39-41.

APPENDIX A
IDEAL-FLUID FLOW CALCULATIONS ABOVE AN INFLATED FLEXIBLE MEMBRANE DAM

For overflow situations above inflated IFMD, the overflowing nappe is subjected to the gravity force, the reaction force of the membrane wall and to an "adherence force" caused by Coanda effect. For small overflows, critical flow conditions take place at the dam crest (i.e. x = 0, y = D, fig. 5) :

$$\frac{d_c}{R} = \frac{2}{3} * \left(\frac{H_1}{R} - \frac{D}{R} \right) \qquad \text{(A1)}$$

where $F_c = V_c / \sqrt{g * R}$, d_c is the critical flow depth, D is the dam height, R is the radius of curvature, V_c is the critical flow velocity, g is the gravity constant and H_1 is the upstream total head (fig. 5). Equation (A1) can be refined by introducing a discharge coefficient.

Assuming a circular shape of the downstream face of the dam, the continuity and momentum equation can be solved to give an expression of the flow depth d and flow velocity V :

$$F = \sqrt{F_c^2 + 2 * (1 - \cos\phi)} \qquad \text{(A2)}$$

$$\frac{d}{R} = \frac{d_c}{R} * \sqrt{\frac{1}{1 + 2 * \frac{1 - \cos\phi}{F_c^2}}} \qquad \text{(A3)}$$

where $F = V / \sqrt{g * R}$ and ϕ is the angular position with ϕ = 0 at the crest (fig. 5).

On the downstream surface of the dam membrane. the pressure distribution may be deduced from the motion equation. At any position ϕ and assuming no radial velocity component, the motion equation in the radial direction is:

$$-\frac{V^2}{g * R} * \frac{d}{R} = \frac{P_s - P_{atm}}{\rho_w * g * R} - \frac{d}{R} * \cos\phi * \left(1 + \frac{d}{2 * R} \right) \qquad \text{(A4)}$$

where P_s is the absolute pressure at the surface of the cylinder, P_{atm} is the atmospheric pressure and ρ_w is the water density. And the dimensionless pressure distribution at the wall becomes :

$$\frac{P_{atm} - P_s}{\rho_w * g * R} = \frac{d}{R} * \left(F^2 - \cos\phi * \left(1 + \frac{d}{2 * R} \right) \right) \qquad \text{(A5)}$$

In equation (A5) F and d/R are deduced from equations (A2) and (A3). Figure 6 presents typical dimensionless pressure distributions for various overflow situations.

H CHANSON

Dr Chanson is a Senior Lecturer in Fluid Mechanics, Hydraulics and Environmental Engineering at the Department of Civil Engineering, The University of Queensland. His research interests include experimental investigations of multiphase flows and particularly air-water mixtures, design of hydraulic and coastal structures and modelling of water quality in rivers, estuaries and the ocean. He wrote two books (*Hydraulic Design of Stepped Cascades, Channels, Weirs and Spillways*, Pergamon, 1995 and *Air Bubble Entrainment in Free-surface Turbulent Shear Flows*, Academic Press, 1997) and over sixty five international refereed journal papers.